Functionalization of Silica Nanoparticles via the Combination of Surface-Initiated RAFT Polymerization and Click Reactions

Yu Li[†] **and Brian C. Benicewicz**[*,‡]

NYS Center for Polymer Synthesis, Department of Chemistry and Chemical Biology, Rensselaer Polytechnic Institute, Troy, New York 12180, and Department of Chemistry and Biochemistry, USC NanoCenter, University of South Carolina, Columbia, South Carolina 29208

Received July 9, 2008; Revised Manuscript Received September 4, 2008

ABSTRACT: A functional monomer with a pendant azide moiety, 6-azidohexyl methacrylate (AHMA), was polymerized on the surface of silica nanoparticles via surface-initiated reversible addition−fragmentation chain transfer (RAFT) polymerization with considerable control over the molecular weight and molecular weight distribution. The kinetics of AHMA polymerization mediated by 4-cyanopentanoic acid dithiobenzoate (CPDB) anchored nanoparticles was investigated and compared with that of AHMA polymerization mediated by free CPDB under similar conditions. The subsequent postfunctionalizations of PAHMA-grafted nanoparticles were demonstrated by reacting with various functional alkynes via click reactions. Kinetic studies showed that the reaction of surface-grafted PAHMA with phenylacetylene surface-grafted PAHMA was much faster than that of free PAHMA with phenylacetylene, whereas in the case of high molecular weight alkynes surface-grafted PAHMA showed lower reaction rates as compared to free PAHMA.

Introduction

Reversible addition−fragmentation chain transfer (RAFT) polymerization, a recently developed controlled radical polymerization (CRP) technique, has been widely used to prepare polymer materials with predetermined molecular weights, narrow polydispersities, and advanced architectures.[1−4] RAFT polymerization is performed under mild conditions, is applicable to a wide range of monomers and does not require a catalyst. Because of these advantages, RAFT polymerization has emerged as one of the most versatile CRP techniques. Recently, the copper-catalyzed Huisgen dipolar cycloadditions, also termed "click reactions", has drawn a great deal of attention due to their high efficiency, technical simplicity, and high specificity.[5−7] Combining click reactions with RAFT polymerization creates a versatile postfunctionalization strategy to prepare highly functionalized polymers. Generally, this postfunctionalization strategy is utilized in two approaches to prepare end-functionalized and side-functionalized polymers. In the first approach, a RAFT agent containing azide or alkyne moiety is prepared and used to mediate the polymerization of various monomers. The resulting polymers contain terminal alkynyl or azido functionalities, which can be used in click reactions with functional azides or alkynes, respectively. Using this approach, Gondi et al. synthesized functional telechelic polymers.[8] Quemener et al. synthesized block copolymers by cojoining azide and alkyne end-functionalized polymer pairs.[9] In the other approach, a polymer with pendant alknyl or azido groups is first synthesized by RAFT polymerization, which is subsequently side-functionalized via click reactions. O'Reilly et al. reported the synthesis of block copolymers incorporating alkyne functionality in the hydrophobic block using RAFT polymerization.[10] These alkyne-functionalized block polymers were used to prepare shell-cross-linked micelles which could be functionalized with azides. Quemener et al. synthesized a comb polymer via RAFT polymerization of a protected alkyne and subsequent click functionalization.[11] In our recent work, we reported the direct polymerization of 2-azidoethyl methacrylate by the RAFT polymerization, and the resulting side functionalization of the azide polymer via click reactions with high efficiency.[12]

Surface modification of nanoparticles with synthetic polymers is of great interest due to their potential application in optics, electronics, and engineering.[13−15] The recent development of the RAFT polymerization technique has proved to be a versatile tool to modify the nanoparticle surfaces with a variety of functional polymers.[16] Among various approaches based on the RAFT technique, surface-initiated RAFT polymerization is arguably the most promising one due to its ability to precisely control the structure of the grafted polymer chains with a low-to-high range of graft densities. Generally, there are two routes to utilize surface-initiated RAFT polymerization to prepare surface-grafted polymer chains including using (1) a surface-anchored initiator with free RAFT agent in solution and (2) a surface-anchored RAFT agent with appropriate initiation method. Tsujii et al.[17] reported the first application of surface-initiated RAFT polymerization in the modification of silica particles using a surface-anchored RAFT agent. Baum and Brittain[18] utilized RAFT to graft polystyrene (PS) and poly(methyl methacrylate) (PMMA) from silica particles using a surface-anchored azo initiator. Since these pioneering works, the surface-initiated RAFT technique has been utilized in the surface modification of various nanoparticles with a wide range of polymers.[19−34] In the recent works of Ranjan and Brittain,[35,36] surface-initiated RAFT polymerization was also combined with click chemistry to modify the surface of silica nanoparticles. In their process, an alkyne-terminated RAFT agent was immobilized onto azide-functionalized silica nanoparticles with high efficiency via click reactions. Using these surface-anchored RAFT agents, high-density polymer brushes could be synthesized on silica nanoparticles.

In an effort to further expand the versatility of surface-initiated RAFT polymerization toward the surface modification of nanoparticles, herein we report a postfunctionalization approach of combining surface-initiated RAFT polymerization and click reactions for nanoparticle functionalization. A functional monomer with a pendent azido group was polymerized on the silica nanoparticle surfaces via surface-initiated RAFT polymerization. The resulting polymer-grafted nanoparticles have a large number of reactive azido groups on them, which can be referred to as

* To whom correspondence should be addressed.
[†] Rensselaer Polytechnic Institute.
[‡] University of South Carolina.

10.1021/ma801551z CCC: $40.75
Published on Web 10/10/2008

"massively reactive nanoparticles". The subsequent postfunctionalizations were demonstrated by reacting with various functional alkynes.

Experimental Section

Materials. Unless otherwise specified, all chemicals were purchased from Acros and used as received. 4-Cyanopentanoic acid dithiobenzoate (CPDB) anchored silica nanoparticles, prop-2-ynyl 4-cyano-4-(phenylcarbonothioylthio)pentanoate, and 4-(4-(phenylamino)phenylamino)phenol were prepared according to the literature.[27,37,38] 2,2′-Azobis(4-methoxy-2,4-dimethylvaleronitrile) (V-70) was purchased from Wako and used as received.

Instrumentation. NMR spectra were recorded on a Varian 500 spectrometer using d_8-THF as solvent. Molecular weights and molecular weight distributions were determined using a Waters gel-permeation chromatograph equipped with a 515 HPLC pump, a 2410 refractive index detector, and three Styragel columns (HR1, HR3, HR4 in the effective molecular weight range of 100−5000, 500−30 000, and 5000−500 000, respectively) with THF as eluent at 30 °C and a flow rate of 1.0 mL/min. The GPC system was calibrated with poly(methyl methacrylate) and polystyrene standards obtained from Polymer Laboratories. Powder conductivity measurement was performed in a custom-built guarded cell, which has electrode size of 1.4 cm in diameter. The cell was connected to a Keithley 6485 picoammeter and a Bertan 225 voltage source during measurement.

Synthesis of 1-Azido-6-hydroxyhexane. To a 250 mL round-bottom flask was added 1-chloro-6-hydroxyhexane (13.65 g, 0.1 mol) and sodium azide (13 g, 0.2 mol) in 50 mL of water. The mixture was stirred at 80 °C for 12 h and then cooled to room temperature. The solution was extracted with ether (3 × 100 mL), dried with sodium sulfate overnight, and filtered. After the removal of the solvent under vacuum, 1-azido-6-hydroxyhexane was obtained as a colorless liquid (yield: 12.9 g, 90%). ^{1}H NMR (500 MHz, $CDCl_3$): δ (ppm) 1.4 (m, 4H, CH_2), 1.53−1.62 (m, 4H, CH_2), 3.26 (t, 2H, CH_2N_3), 3.64 (t, 2H, CH_2O).

Caution: special care should be taken to minimize the possible explosion in the preparation and handling of the azide compound.

Synthesis of 6-Azidohexyl Methacrylate (AHMA). To a 500 mL round-bottom flask, a solution of 1-azido-6-hydroxyhexane (14.3 g, 100 mmol), methacrylic acid (7.74 g, 90 mmol), and 4-(dimethylamino)pyridine (DMAP) (3.67 g, 30 mmol) in 100 mL of methylene chloride was cooled to 0 °C. Dicyclohexylcarbodiimide (DCC) (20.63 g, 100 mmol) was dissolved in 50 mL of methylene chloride and added slowly to the solution. The resulting mixture was warmed to room temperature and stirred overnight. The precipitate was removed by filtration. After removal of solvent and silica gel column chromatography (10:1 mixture of hexane and ethyl acetate), the product was obtained as a colorless liquid (yield: 16.1 g, 85%). ^{1}H NMR (500 MHz, $CDCl_3$): δ (ppm) 1.41 (m, 4H, CH_2), 1.59−1.72 (m, 4H, CH_2), 1.95 (s, 3H, CH_3C), 3.26 (t, 2H, CH_2N_3), 4.15 (t, 2H, CH_2O), 5.55 (s, 1H, =CH), 6.1 (s, 1H, =CH). ^{13}C NMR (500 MHz, $CDCl_3$): 18.79, 26.07, 26.85, 28.96, 29.21, 51.8, 64.98, 125.71, 136.8, 167.9. IR (NaCl disk): 1720 cm^{-1} (C=O) and 2100 cm^{-1} (N_3).

Graft Polymerization of AHMA from CPDB Anchored Silica Nanoparticles. A solution of AHMA (0.5 g), CPDB anchored silica (0.15 g, 28 μmol/g), V-70 (0.45 μmol), and THF (3 mL) was prepared in a dried Schlenk tube. The mixture was degassed by three freeze−pump−thaw cycles, backfilled with nitrogen, and then placed in an oil bath at 30 °C for various intervals. The polymerization was quenched in ice water. A small amount of polymerization solution was withdrawn to measure monomer conversion by NMR. The polymer solution was precipitated into methanol, filtered, and dried under vacuum. A monomer conversion of 5% was reached after 6 h. The cleaved PAHMA had a number-average molecular weight of 7600 and a PDI of 1.2.

Monomer conversion for AHMA was calculated based on the following equation:

$$C_{\mathrm{AHMA}} = \frac{I_{0.6-1}}{I_{0.6-1} + 3I_{5.4-5.5}}$$

where $I_{0.6-1}$ is the integrated area of the signal for the methyl protons of the polymer and $I_{5.4-5.5}$ is the integrated area of the signal for one of the olefinic protons of the monomer.

Synthesis of SiO_2-*graft*-(PAHMA-*block*-PMMA). A solution of SiO_2-*graft*-PAHMA ($M_{\mathrm{n(cleaved\ PAHMA)}}$ = 7600, PDI = 1.2) (100 mg), methyl methacrylate (0.5 mL, 2 mmol), V-70 (0.225 μmol), and THF (1 mL) was prepared in a dried Schlenk tube. The mixture was degassed by three freeze−pump−thaw cycles, backfilled with nitrogen, and then placed in a 30 °C oil bath. After 4 h, the polymerization solution was quenched in ice water and poured into an aluminum boat. The solvent and monomer were removed by evaporation in a fume hood overnight and then 2 days under vacuum to determine monomer conversion by gravimetric analysis, and molecular weight characteristics were analyzed by GPC after cleavage from the silica nanoparticles (conversion = 15%, $M_{\mathrm{n(cleaved\ PAHMA\text{-}}b\text{-PMMA)}}$ = 24 000, PDI = 1.24).

Cleavage of Grafted PAHMA from Silica Nanoparticles. PAHMA (20 mg) grafted silica nanoparticles were dissolved in THF (4 mL). HF (0.5 mL, 49% in aq) and phase transfer agent Aliquat 336 (20 mg) were added, and the solution was allowed to stir at room temperature overnight. The solution was poured into a PTFE Petri dish and allowed to stand in a fume hood overnight to evaporate the volatiles. The recovered PAHMA was dissolved in THF, passed through neutral alumina, and then subjected to GPC analysis.

Synthesis of Alkyne-Terminated Oligoaniline (ALOAN). To a 100 mL round-bottom flask, a solution of 4-(4-(phenylamino)phenylamino)phenol (2.76 g, 10 mmol) and triethylamine (10.1 g, 11 mmol) in 50 mL of methylene chloride was cooled to 0 °C. Propargyl chloroformate (1.3 g, 11 mmol) was added slowly to the solution. The resulting mixture was warmed to room temperature and stirred overnight. The precipitate was removed by filtration. After removal of solvent and silica gel column chromatography (3:1 mixture of hexane and ethyl acetate), the product was obtained as a gray solid (yield: 3 g, 85%); mp: 84 °C (capillary uncorrected). ^{1}H NMR (500 MHz, DMSO-d_6): δ (ppm) 3.7 (s, 1H, CH), 4.85 (s, 2H, CH_2), 6.7 (t, 1H, aromatic), 6.8−7.2 (m, 12H, aromatic), 7.9 (s, 1H, NH), 8.0 (s, 1H, NH). ^{13}C NMR (500 MHz, DMSO-d_6): 56.5, 78.3, 79.6, 115.9, 116, 119.1, 120.3, 120.6, 122.4, 129.8, 136.8, 137.5, 143.3, 144, 145.5, 153.8.

Synthesis of Alkyne-Terminated Polystyrene (ALPS). A solution of styrene (9 mL), prop-2-ynyl 4-cyano-4-(phenylcarbonothioylthio)pentanoate (0.3 g), and AIBN (12 mg) was prepared in a dried Schlenk tube. The mixture was degassed by three freeze−pump−thaw cycles, backfilled with nitrogen, and then placed in an oil bath at 60 °C for 13 h. The polymerization solution was quenched in ice water and precipitated into cold methanol. The polymer was recovered by centrifugation and dried under vacuum (M_n = 1000, PDI = 1.05).

Click Functionalization of PAHMA Grafted Silica Nanoparticles. A mixture of PAHMA grafted silica nanoparticles (1 equiv of $-N_3$), alkyne (2 equiv), and *N*,*N*,*N*′,*N*″,*N*″-pentamethyldiethylenetriamine (PMDETA) (0.5 equiv) was dissolved in deuterated THF. The solution was degassed by bubbling nitrogen for 5 min and transferred to a NMR tube containing CuBr (0.5 equiv) under a nitrogen atmosphere. The reactions were conducted at room temperature and monitored by ^{1}H NMR spectroscopy. After reaction, the mixture was diluted with THF and passed through neutral alumina to remove the copper catalyst. After concentration by rotary evaporation, the solution was precipitated into methanol (cyclohexane for reaction with ALPS) to remove residual alkyne. After filtration, the product was dried under vacuum.

Results and Discussion

RAFT Polymerization. The azido-containing monomer, AHMA, was synthesized by a two-step reaction. 1-Azido-6-

Scheme 1. Synthesis of PAHMA Grafted Silica Nanoparticles and Click Functionalization

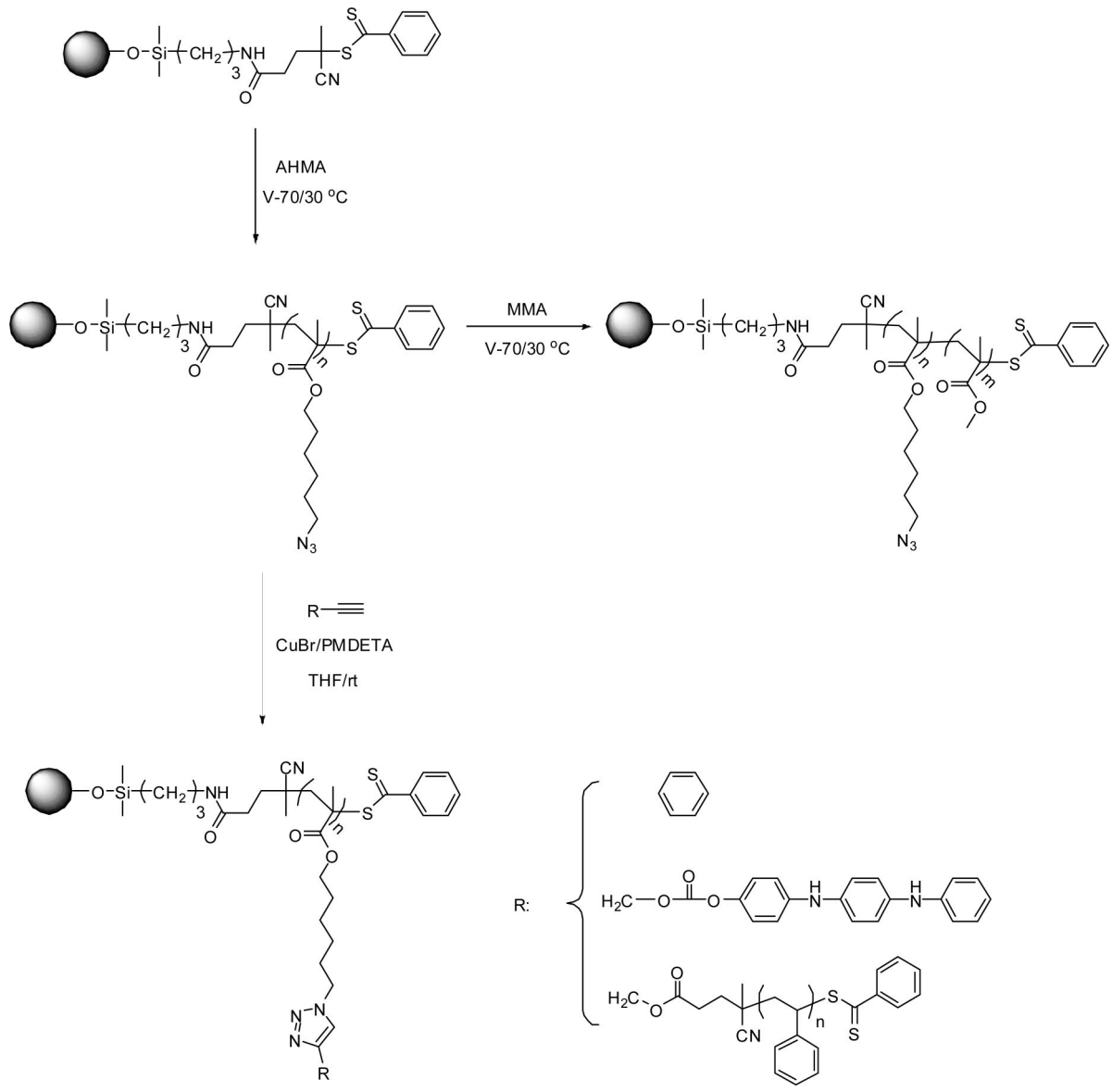

hydroxyhexane was first prepared by reacting 1-chloro-6-hydroxyhexane with sodium azide. The subsequent DCC/DMAP mediated coupling of methacrylic acid and 1-azido-6-hydroxyhexane gave the product in good yield under mild reaction conditions. The CPDB anchored silica nanoparticles, NP-1 and NP-2, were prepared according to the literature,[27] which had surface densities of 28 and 76 μmol/g. Considering the side reactions occurring with the azido group at elevated temperatures, the surface-initiated RAFT polymerization of AHMA was conducted at the relatively low temperature of 30 °C using V-70 as a radical initiator (Scheme 1). To minimize the free polymer in solution, a high CPDB to V-70 ratio (10) was utilized, and the monomer conversion was also limited to less than 30%. The surface graft polymerizations of AHMA mediated by the CPDB anchored silica nanoparticles with two surface densities were conducted under identical reaction conditions for comparison. To investigate the difference between the polymerization behavior on the surface of nanoparticles and that in solution, the RAFT polymerization of AHMA in solution mediated with free CPDB was also conducted under identical reaction conditions.

Figure 1 shows the GPC traces for the RAFT polymerization of AHMA mediated with free CPDB and CPDB anchored nanoparticles with two different surface densities. For the polymerization of AHMA mediated by free CPDB and NP-1, the GPC traces were observed to be narrow and unimodal over the range of conversions investigated in this study. However, in the case of the AHMA polymerization mediated by NP-2, a slight high molecular weight shoulder was observed even at very low conversion. This high molecular weight shoulder became more distinguishable with the increase of conversion and finally resulted in an obvious broadening of the GPC trace. In recent work,[12] we have demonstrated that the azido group could cycloadd to methacrylate monomer during the RAFT polymerization of the azide monomer, which leads to the branching of polymer chains, represented by the appearance of a high molecular weight shoulder on the GPC trace. For the surface-initiated RAFT polymerization of AHMA mediated by CPDB anchored nanoparticles, the polymer chains are growing from the reactive sites on the nanoparticle surfaces. Because of the immobilization of the polymer chains, the local concentration of polymer chains on the nanoparticle surfaces is very high, which results in the extremely high concentration of azido groups near the nanoparticle surfaces. Because the grafted polymer chains will not strongly hinder the diffusion of small-sized monomer to the surface, AHMA monomer will have a

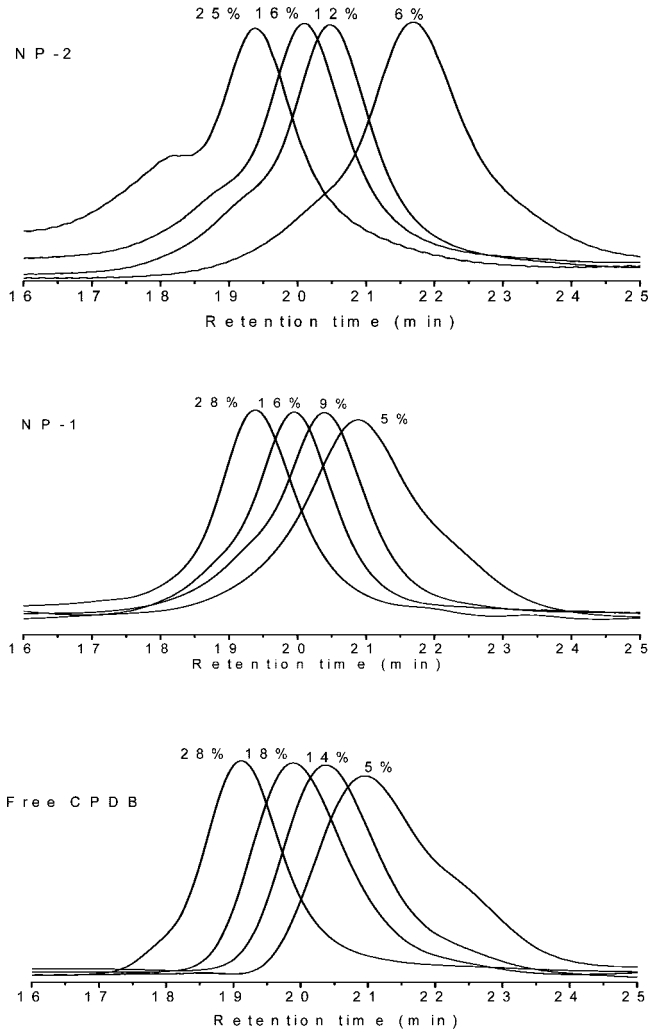

Figure 1. GPC traces for the RAFT polymerization of AHMA ([AHMA] = 0.7 M, [V-70] = 1.12×10^{-4} M, 30 °C) mediated with free CPDB and CPDB anchored nanoparticles: low density (NP-1) (28 μmol/g, 1.12×10^{-3} M); high density (NP-2) (76 μmol/g, 1.12×10^{-3} M).

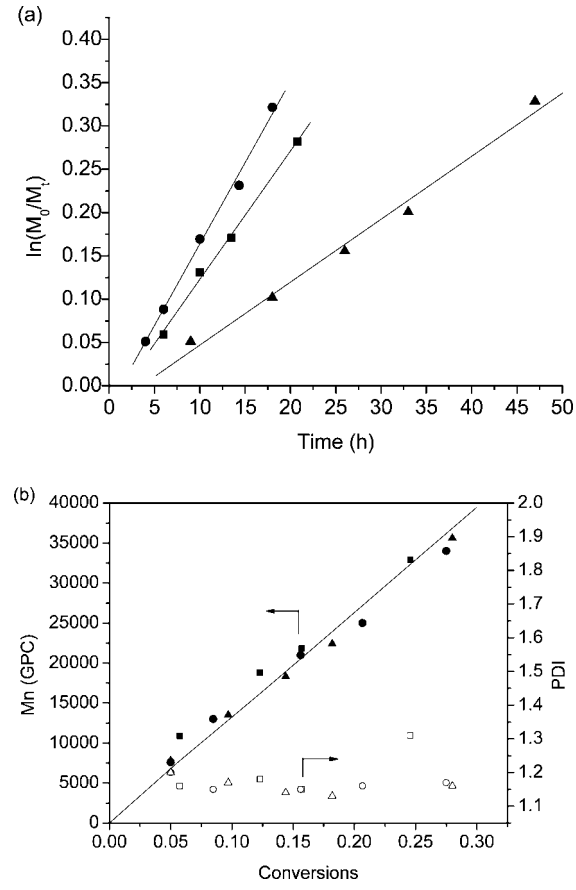

Figure 2. (a) Kinetic plots and (b) dependence of the molecular weight and polydispersity on conversion for the RAFT polymerization of AHMA ([AHMA] = 0.7 M, [V-70] = 1.12×10^{-4} M, 30 °C) mediated with free CPDB (1.12×10^{-3} M, triangle) and CPDB-anchored nanoparticles: low density (NP-1) (28 μmol/g, 1.12×10^{-3} M, circle); high density (NP-2) (76 μmol/g, 1.12×10^{-3} M, square). Solid line in (b) is the theoretically calculated molecular weight.

great probability to be involved in the side reaction with the azido group on the grafted polymer chains before adding to propagating radicals or diffusing out. This concentration effect becomes more obvious with the increase of both the graft density and molecular weight of the grafted polymer chains, which is a likely reason for the appearance of high molecular weight shoulders for the polymerization of AHMA mediated by NP-2.

The kinetic results for the RAFT polymerization of AHMA mediated by CPDB anchored nanoparticles and free CPDB at 30 °C are shown in Figure 2a. A linear relationship between $\ln(M_0/M_t)$ (where M_0 is the initial monomer concentration and M_t is the monomer concentration at time t) and polymerization time was observed for all three cases, indicating a constant radical concentration during the polymerization. The polymerization mediated by NP-1 was slightly faster that the polymerization mediated by NP-2, and a longer induction period was also observed for the NP-2 system. This phenomenon is consistent with the results of the styrene and butyl acrylate surface polymerizations in the literature,[19] which could be ascribed to the "localized high RAFT agent concentration" effect. However, compared to the polymerization mediated by free CPDB, the polymerizations mediated by CPDB-anchored nanoparticles were significantly faster, which cannot be explained by the "localized high RAFT agent concentration" effect. In a previous paper,[27] it was reported that the polymerization of methyl methacrylate on the nanoparticle surfaces was much faster that that in solution, which was speculated to be attributed to the unique steric environment of the intermediate macro-RAFT agent radical on the nanoparticle surfaces. Because of the structure similarity between AHMA and methyl methacrylate, the similar results observed for the surface polymerization of AHMA further supports this speculation.

The controlled nature of AHMA polymerization was demonstrated by the linear increase in M_n with monomer conversion as shown in Figure 2b. It is noted that the measured molecular weight for all three cases had a close agreement with the theoretical molecular weight (represented by the solid line in Figure 2b), which indicated a high efficiency of free CPDB as well as anchored CPDB throughout the polymerization. For the polymerization of AHMA mediated by free CPDB and NP-1, the molecular weight distribution remained narrow (<1.2) over the range of conversions investigated. Although well-defined polymer chains were obtained (PDI < 1.2) at conversions <20% in the case of NP-2, an increase in PDI (1.31) was observed at higher conversion (25%), corresponding to the appearance of the high molecular weight shoulder in the GPC trace.

The surface-initiated RAFT technique has particular utility in the preparation of surface-grafted block copolymers. The ability to form block copolymers by the chain extension is also an excellent indication of the "living" characteristics of the homopolymer grafted from the surface of nanoparticles. In this work, an NP-1-*graft*-PAHMA ($M_{n(\text{cleaved PAHMA})}$ = 7600, PDI = 1.2) was first prepared with a monomer conversion of 5%.

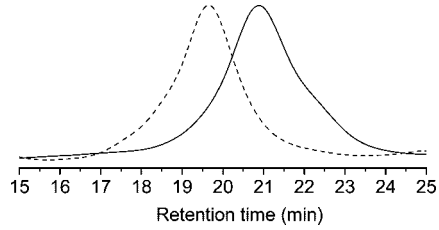

Figure 3. GPC traces for NP-1-*graft*-PAHMA ($M_{n(cleaved\ PAHMA)}$ = 7600, PDI = 1.2, solid) and NP-1-*graft*-(PAHMA-*block*-PMMA) ($M_{n(cleaved\ PAHMA\text{-}b\text{-}PMMA)}$ = 24 000, PDI = 1.24, dashed).

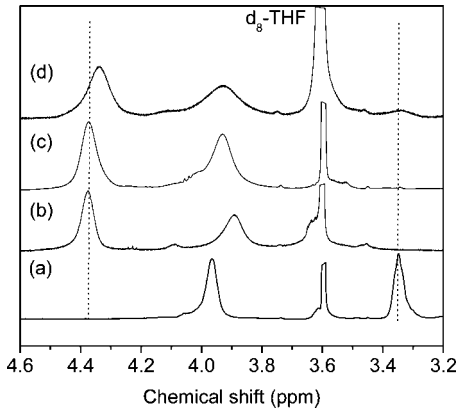

Figure 4. ^{1}H NMR spectra of (a) PAHMA, (b) PAHMA-*click*-phenylacetylene, (c) PAHMA-*click*-ALOAN, and (d) PAHMA-*click*-ALPS.

The isolated NP-1-*graft*-PAHMA was employed as macroCTA for polymerization of MMA to produce a block copolymer, NP-1-*graft*-(PAHMA-*block*-PMMA). The MMA conversion was 15% after 4 h at 30 °C. As shown in Figure 3, the complete shift of the GPC trace and the low polydispersity of the cleaved block copolymer ($M_{n(cleaved\ PAHMA\text{-}b\text{-}PMMA)}$ = 24 000, PDI = 1.24) demonstrated the controlled nature of the polymerization and the fidelity of the end-group functionalities.

Click Functionalization. The polymer chains with pendant azido groups can be side-functionalized with alkynes via the highly efficient click reaction. The above-prepared PAHMA-grafted nanoparticles have a large number of reactive azido groups on the grafted PAHMA chains, which are excellent precursors for attaching various functional alkynes. However, since PAHMA chains are immobilized on the surface of nanoparticles, the efficiency of click functionalization might be significantly decreased due to the large steric hindrance introduced by the localized high polymer chain concentration. To compare the click efficiency of grafted PAHMA with that of free PAHMA, three alkynes with different molecular weights, including phenylacetylene, ALOAN, and ALPS, were selected to be reacted with both grafted PAHMAs and free PAHMA in THF using CuBr/PMDETA as catalyst. Figure 4 shows the ^{1}H NMR spectra of PAHMA and click functionalized PAHMAs. It was observed that the signal (3.3−3.4 ppm) from $-CH_2N_3$ protons of PAHMA was shifted quantitatively downfield (4.3−4.4 ppm) upon triazole formation, which could be monitored over time to determine the conversion of azido groups. The dependence of conversion on time for the reaction of phenylacetylene with PAHMA, NP-1-*graft*-PAHAM, and NP-2-*graft*-PAHMA is shown in Figure 5. Surprisingly, for grafted PAHMAs more than 90% conversions were achieved in 20 min, which was much faster than that for free PAHMA under identical conditions. A possible reason for this unexpectedly high rate of reaction could be the concentration effect. For surface grafted PAHMA, the local concentration of azido groups

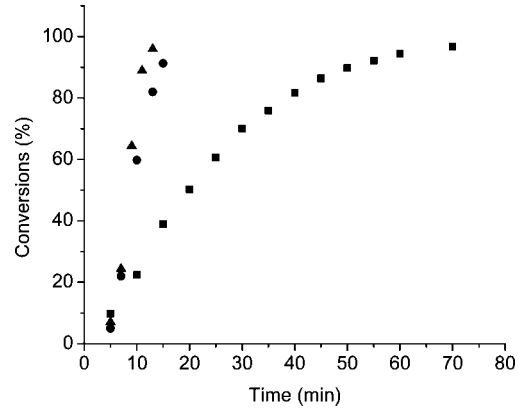

Figure 5. Dependence of conversion on time for the reaction of phenylacetylene with PAHMA (M_n = 9500, PDI = 1.1, square), NP-1-*graft*-PAHMA ($M_{n(cleaved\ PAHMA)}$ = 9400, PDI = 1.16, circle), and NP-2-*graft*-PAHAM ($M_{n(cleaved\ PAHMA)}$ = 9800, PDI = 1.18, triangle). Experimental conditions: [$-N_3$] = 0.05 M; [$-N_3$]:[$-C\equiv CH$]:[CuBr]:[PMDETA] = 1:2:0.5:0.5; in THF-d_8 monitored by ^{1}H NMR spectroscopy at room temperature.

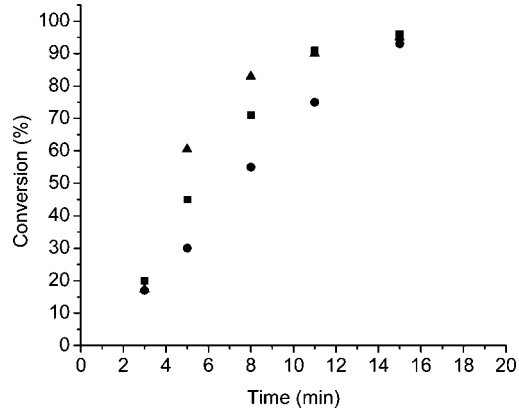

Figure 6. Dependence of conversion on time for the reaction of ALOAN with PAHMA (M_n = 9500, PDI = 1.1, square), NP-1-*graft*-PAHMA ($M_{n(cleaved\ PAHMA)}$ = 9400, PDI = 1.16, circle), and NP-2-*graft*-PAHAM ($M_{n(cleaved\ PAHMA)}$ = 9800, PDI = 1.18, triangle). Experimental conditions: [$-N_3$] = 0.05 M; [$-N_3$]:[$-C\equiv CH$]:[CuBr]:[PMDETA] = 1:2:0.5:0.5; in THF-d_8 monitored by ^{1}H NMR spectroscopy at room temperature.

near the nanoparticle surfaces is much higher than the normal concentration of azido groups for free PAHMA in solution. Once alkyne diffuses into the grafted PAHMA chains, it will be consumed quickly by reacting with an azido group to form a triazole. With the consumption of alkyne, the concentration of azido groups decreases while the local concentration of triazoles increases correspondingly. Because of the exceptional ability of triazoles to bind and stabilize copper(I),[39,40] the local concentration of copper(I) catalyst increases dramatically, which further boosts the conversion of remaining azido groups. Therefore, these PAHMA-grafted nanoparticles can be actually regarded as "massively reactive nanoparticles", which can be functionalized by trapping and reacting with alkynes with very high efficiency. For phenylacetylene, its diffusion is not severely hindered by the grafted PAHMA chains due to the relatively small size, which leads to the high reaction rate. To further study the effect of the size of the alkyne on the rate of click reaction, kinetics for the cases of two large-sized alkynes, ALOAN and ALPS, were also investigated. As shown in Figures 5 and 6, the reaction of ALOAN with free PAHMA was much faster than that of phenylacetylene with free PAHMA, which may be attributed to the higher reactivity of ALOAN. For grafted PAHMAs, although the larger size of ALOAN compared to

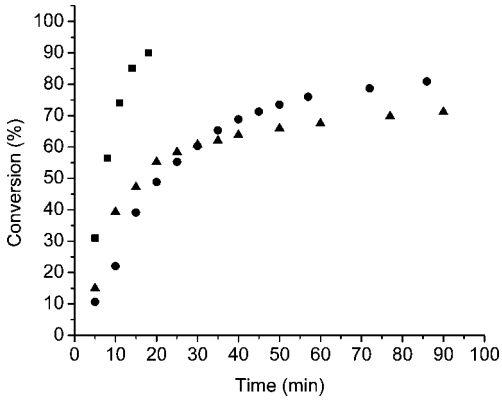

Figure 7. Dependence of conversion on time for the reaction of ALPS (M_n = 1000, PDI = 1.06) with PAHMA (M_n = 9500, PDI = 1.1, square), NP-1-*graft*-PAHMA ($M_{n(cleaved\ PAHMA)}$ = 9400, PDI = 1.16, circle), and NP-2-*graft*-PAHAM ($M_{n(cleaved\ PAHMA)}$ = 9800, PDI = 1.18, triangle). Experimental conditions: [$-N_3$] = 0.05 M; [$-N_3$]:[$-C\equiv CH$]:[CuBr]:[PMDETA] = 1:2:0.5:0.5; in THF-d_8 monitored by ^{1}H NMR spectroscopy at room temperature.

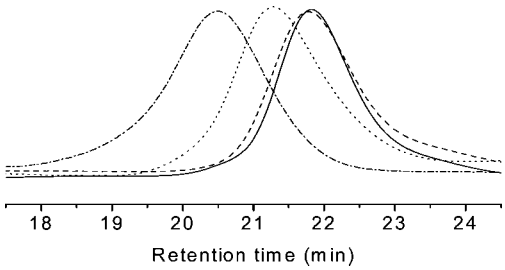

Figure 8. GPC traces of (a) PAHMA (M_n = 9500, $M_{n,theor}$ = 8500, PDI = 1.1, solid), (b) PAHMA-*click*-phenylacetylene (M_n = 9400, $M_{n,theor}$ = 13 100, PDI = 1.11, dash), (c) PAHMA-*click*-ALOAN (M_n = 14500, $M_{n,theor}$ = 24 600, PDI = 1.12, dot), and (d) PAHMA-*click*-ALPS (M_n = 20 400, $M_{n,theor}$ = 53 500, PDI = 1.18, dash-dot).

phenylacetylene might be expected to lead to the increased steric hindrance, its higher reactivity resulted in reaction rates at the same level as those of phenylacetylene. For the case of the bulky ALPS, the click efficiency of grafted PAHMAs was significantly decreased (Figure 7). At conversions <50% the rates of click reactions for grafted PAHMAs were still comparable to that for free PAHMA. However, significant drops of the reaction rates for grafted PAHMAs, particularly NP-2-*graft*-PAHAM, which has the highest surface graft density, were observed at higher conversions, indicating that the steric hindrance created by the grafted particles and molecular weight of the alkyne had a effect on the rate of click reactions.

After the click reaction, attempts were made to cleave the functionalized polymers from the nanoparticle surfaces by treating with HF. However, degrafting of the polymer was extremely difficult as the nanoparticles precipitated from THF solution immediately after the addition of HF, which may be attributed to the protonation of triazole rings on the grafted polymer chains. The functionalized polymers prepared from free PAHMAs were analyzed by GPC to examine the molecular weight changes of the postfunctionalized polymers. As shown in Figure 8, the molecular weight distributions of the functionalized polymers after the click functionalization remained very low (<1.2), indicating the high fidelity of click reaction. No obvious shift of the GPC trace was observed upon the click functionalization of PAHMA with phenylacetylene, which is similar to the result reported in a previous paper[10] for the click functionalization of PAZMA with phenylacetylene. For PAHMA-*click*-ALOAN and PAHMA-*click*-ALPS, their apparent molecular weights were higher than those of the PHEMA precursors

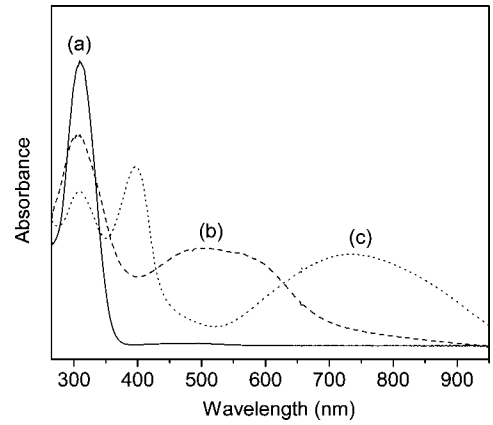

Figure 9. UV−vis spectra of ALOAN-functionalized NP-2-*graft*-PAHAM ($M_{n(cleaved\ PAHMA)}$ = 18 800, PDI = 1.18) in DMF solution: (a) reduced, (b) oxidized, and (c) doped with sulfuric acid.

but still much lower than the theoretical values, which could be ascribed to the changes in the hydrodynamic volume of the polymer chains in solution upon functionalization.

One of the primary advantages of the postfunctionalization strategy is the ability to prepare novel functional polymers by incorporating functionality that is incompatible with the polymerization conditions. For example, it is known that interesting electrical and electrochemical properties can be introduced by incorporating conjugated aniline oligomers into polymer structures.[41] However, direct free radical polymerization of monomer containing oligoaniline moieties is difficult due to the radical-inhibiting ability of the diphenylamine unit. To demonstrate the benefits of the high efficiency and fidelity of click reaction, the side chains of PAHMA grafted on the nanoparticle surfaces were completely functionalized by reacting with an alkyne containing oligoaniline, ALOAN, giving ALOAN-functionalized nanoparticles with well-defined structure. Figure 9 shows the UV−vis spectra of the resulting ALOAN-functionalized nanoparticles recorded in DMF solution. It was observed that the ALOAN-functionalized nanoparticles showed redox properties which were similar to those of the oligomeric aniline.[42] In the reduced state the functionalized nanoparticles exhibited a single strong absorption at 310 nm of the UV−vis spectrum, ascribed to the $\pi-\pi^*$ transition in the benzenoid ring of attached oligoaniline side chains. After oxidizing the nanoparticle solution by bubbling oxygen, a sharp peak at 308 nm and a broad peak at 450−650 nm were observed. The broad peak was attributed to the benzenoid to quinoid excitonic transition. When the oxidized nanoparticle solution was doped with sulfuric acid, three peaks were displayed in the UV−vis spectrum at 308, 400, and 750 nm, and the nanoparticles remained in solution. The protonation of the oxidized oligoaniline units on the nanoparticle surfaces caused the low wavelength absorption to split. The high wavelength absorption red-shifted and extended toward the near-IR region. The electrical conductivity of ALOAN-functionalized nanoparticles was also measured. The powdered sample were first doped with iodine vapor for 1 week and then pressed into a pellet. The measurement of conductivity was performed at room temperature in a laboratory atmosphere. The conductivity of ALOAN-functionalized NP-2-*graft*-PAHAM ($M_{n(cleaved\ PAHMA)}$ = 18 800, PDI = 1.18) was measured to be 1×10^{-5} S/cm, which is in the semiconducting range.

Conclusions

A postfunctionalization approach of combining surface-initiated RAFT polymerization and click reactions to modify the surface of nanoparticles was demonstrated. A functional monomer with a pendant "clickable" moiety, 2-azidoethyl

methacrylate (AHMA), was first polymerized on the nanoparticle surfaces via surface-initiated RAFT polymerization with considerable control over the molecular weight and molecular weight distribution. The rate of AHMA polymerization mediated by CPDB anchored nanoparticles was much higher than that of AHMA polymerization mediated by free CPDB under similar conditions. In the case of AHMA polymerization mediated by CPDB anchored nanoparticles with high surface density, a broadening of the molecular weight distribution was observed at high conversions, indicating that the involvement of the side-chain azido groups in side reactions could be enhanced by the increased density of PAHMA chains on the nanoparticle surface. Retention of the end-group functionality of the grafted PAHMA homopolymer was confirmed by chain extension with methyl methacrylate to yield a narrow-polydispersity diblock copolymer. The subsequent postfunctionalizations of PAHMA-grafted nanoparticles were demonstrated by reacting with various functional alkynes via click reactions. Kinetic studies showed that the reaction of surface-grafted PAHMA with phenylacetylene surface-grafted PAHMA was much faster than that of free PAHMA with phenylacetylene, which was attributed to the localized concentration effect, whereas in the case of high molecular weight alkynes surface-grafted PAHMA showed lower reaction rates as compared to free PAHMA, which was attributed to the large steric hindrance. This strategy of combining surface-initiated RAFT polymerization with click chemistry provides a promising way to modify the nanoparticle surfaces with a wide range of functional polymers, particularly when the pendant moiety may interfere with the polymerization reaction.

Acknowledgment. The authors gratefully acknowledge support through the Nanoscale Science and Engineering Initiative of the National Science Foundation under NSF Award DMR-0117792. The authors also thank X. Wang and D. Dukes for assistance with conductivity measurements.

References and Notes

(1) Chiefari, J.; Chong, Y. K.; Ercole, F.; Krstina, J.; Jeffery, J.; Le, T. P. T.; Mayadunne, R. T. A.; Meijs, G. F.; Moad, C. L.; Moad, G.; Rizzardo, E.; Thang, S. H. *Macromolecules* **1998**, *31*, 5559–5562.
(2) Lowe, A. B.; McCormick, C. L. *Aust. J. Chem.* **2002**, *55*, 367–379.
(3) Moad, G.; Rizzardo, E.; Thang, S. H. *Aust. J. Chem.* **2005**, *58*, 379–410.
(4) Moad, G.; Rizzardo, E.; Thang, S. H. *Aust. J. Chem.* **2006**, *59*, 669–692.
(5) Rostovtsev, V. V.; Green, L. G.; Fokin, V. V.; Sharpless, K. B. *Angew. Chem., Int. Ed.* **2002**, *41*, 2596–2599.
(6) Tornoe, C. W.; Christensen, C.; Meldal, M. *J. Org. Chem.* **2002**, *67*, 3057–3064.
(7) Kolb, H. C.; Finn, M. G.; Sharpless, K. B. *Angew. Chem., Int. Ed.* **2001**, *40*, 2004–2021.
(8) Gondi, S. R.; Vogt, A. P.; Sumerlin, B. S. *Macromolecules* **2007**, *40*, 474–481.
(9) Quemener, D.; Davis, T. P.; Barner-Kowollik, C.; Stenzel, M. H. *Chem. Commun.* **2006**, 5051–5053.
(10) O'Reilly, R. K.; Joralemon, M. J.; Hawker, C. J.; Wooley, K. L. *Chem.—Eur. J.* **2006**, *12*, 6776–6786.
(11) Quemener, D.; Le Hellaye, M.; Bissett, C.; Davis, T. P.; Barner-Kowollik, C.; Stenzel, M. H. *J. Polym. Sci., Part A: Polym. Chem.* **2008**, *46*, 155–173.
(12) Li, Y.; Yang, J. W.; Benicewicz, B. C. *J. Polym. Sci., Part A: Polym. Chem.* **2007**, *45*, 4300–4308.
(13) Gangopadhyay, R.; De, A. *Chem. Mater.* **2000**, *12*, 608–622.
(14) Sun, Y. P.; Riggs, J. E. *Int. Rev. Phys. Chem.* **1999**, *18*, 43–90.
(15) Sanchez, C.; Lebeau, B.; Chaput, F.; Boilot, J. P. *Adv. Mater.* **2003**, *15*, 1969–1994.
(16) Li, Y.; Schadler, L. S.; Benicewicz, B. C. In *Handbook of RAFT Polymerization*; Barner-Kowollik, C., Ed.; Wiley-VCH: Weinheim, Germany, 2008; pp 423−453.
(17) Tsujii, Y.; Ejaz, M.; Sato, K.; Goto, A.; Fukuda, T. *Macromolecules* **2001**, *34*, 8872–8878.
(18) Baum, M.; Brittain, W. J. *Macromolecules* **2002**, *35*, 610–615.
(19) Li, C. Z.; Benicewicz, B. C. *Macromolecules* **2005**, *38*, 5929–5936.
(20) Hu, T. J.; You, Y. Z.; Pan, C. Y.; Wu, C. *J. Phys. Chem. B* **2002**, *106*, 6659–6662.
(21) Raula, J.; Shan, J.; Nuopponen, M.; Niskanen, A.; Jiang, H.; Kauppinen, E. I.; Tenhu, H. *Langmuir* **2003**, *19*, 3499–3504.
(22) Matsumoto, K.; Tsuji, R.; Yonemushi, Y.; Yoshida, T. *J. Nanopart. Res.* **2004**, *6*, 649–659.
(23) Matsumoto, K.; Tsuji, R.; Yonemushi, Y.; Yoshida, T. *Chem. Lett.* **2004**, *33*, 1256–1257.
(24) Skaff, H.; Emrick, T. *Angew. Chem., Int. Ed.* **2004**, *43*, 5383–5386.
(25) Li, C.; Benicewicz, B. C. *Macromolecules* **2005**, *38*, 5929–5936.
(26) Perrier, S.; Takolpuckdee, P.; Mars, C. A. *Macromolecules* **2005**, *38*, 6770–6774.
(27) Li, C.; Han, J.; Ryu, C. Y.; Benicewicz, B. C. *Macromolecules* **2006**, *39*, 3175–3183.
(28) Wang, W. C.; Neoh, K. G.; Kang, E. T. *Macromol. Rapid Commun.* **2006**, *27*, 1665–1669.
(29) Zhao, Y. L.; Perrier, S. *Macromolecules* **2006**, *39*, 8603–8608.
(30) Nguyen, D. H.; Vana, P. *Polym. Adv. Technol.* **2006**, *17*, 625–633.
(31) Chung, P. W.; Kumar, R.; Pruski, M.; Lin, V. S. Y. *Adv. Funct. Mater.* **2008**, *18*, 1390–1398.
(32) Liu, C. H.; Pan, C. Y. *Polymer* **2007**, *48*, 3679–3685.
(33) Zhao, Y.; Perrier, S. *Macromolecules* **2007**, *40*, 9116–9124.
(34) Hong, C. Y.; Li, X.; Pan, C. Y. *Eur. Polym. J.* **2007**, *43*, 4114–4122.
(35) Ranjan, R.; Brittain, W. J. *Macromol. Rapid Commun.* **2008**, *29*, 1104–1110.
(36) Ranjan, R.; Brittain, W. J. *Macromol. Rapid Commun.* **2007**, *28*, 2084–2089.
(37) Li, Y.; Benicewicz, B. C. *Polym. Prepr. (Am. Chem. Soc., Div. Polym. Chem.)* **2007**, *48*, 524–525.
(38) Chen, R.; Benicewicz, B. C. *ACS Symp. Ser.* **2003**, *843*, 126–139.
(39) Chan, T. R.; Hilgraf, R.; Sharpless, K. B.; Fokin, V. V. *Org. Lett.* **2004**, *6*, 2853–2855.
(40) Sumerlin, B. S.; Tsarevsky, N. V.; Louche, G.; Lee, R. Y.; Matyjaszewski, K. *Macromolecules* **2005**, *38*, 7540–7545.
(41) Chen, Y. W.; Ying, L.; Yu, W. H.; Kang, E. T.; Neoh, K. G. *Macromolecules* **2003**, *36*, 9451–9457.
(42) Chen, R.; Benicewicz, B. C. *Synth. Met.* **2004**, *146*, 133–137.

MA801551Z